Surface Enhanced Raman Scattering

DOI: 10.1002/anie.200806139

Isolating and Probing the Hot Spot Formed between Two Silver Nanocubes**

*Pedro H. C. Camargo, Matthew Rycenga, Leslie Au, and Younan Xia**

There has been a renewed interest in surface-enhanced Raman scattering (SERS) after the demonstration of single-molecule detection with substrates made of silver nanoparticles.[1,2] In this system, it is thought that the giant enhancements that allowed for single-molecule detection did not occur homogeneously over the entire substrate. Instead, they occurred only at particular sites, the so-called hot spots.[3] Hot spots can be defined as junctions or gaps between two or more closely spaced particles in which enormous electromagnetic enhancements often arise, in contrast to individual particles.[4] The commonly used method for producing SERS substrates containing hot spots relies on the uncontrolled aggregation of silver or gold nanoparticles as induced by a salt.[5] While these aggregates can provide strong SERS signals, the poor reproducibility of their fabrication as well as the broad size distribution and shape irregularity of the involved silver nanoparticles imposes many challenges for correlating the detected scattering enhancement to the specific feature of a hot spot. Thus, although the hot-spot phenomenon has been extensively investigated from both theoretical and experimental perspectives, it still remains an elusive, feebly understood subject. In this regard, individual dimers of nanoparticles represent an ultimate system for quantitatively investigating the hot-spot phenomenon. At least, they would enable an easier correlation between specific hot-spot structures and the observed SERS intensities.[6–8] Moreover, enhancements strong enough for ultrasensitive analysis and even single-molecule detection have been proposed for dimers consisting of silver nanoparticles.[9] Despite these advantages, there are still limitations associated with the utilization of nanoparticle dimers for studying the hot spot. Owing to the size and shape of the usually employed nanoparticles, SERS molecules absorbed inside and outside the hot-spot region can contribute to the detected SERS intensities.[6–9] As a result, the experimentally determined enhancement factor (EF) represents the average enhancement from the entire surface of the dimer. In this regard, determination of EFs exclusive from the hot-spot region still remains a great challenge.

Herein, we describe a new strategy based on plasma etching for exclusively measuring the SERS signals from those molecules located in the hot-spot region formed between two Ag nanocubes. In this approach, the dimer of Ag nanocubes was functionalized with SERS probe molecules and then briefly exposed to plasma etching to selectively remove those molecules outside the hot-spot region. With the aid of registration marks on the silicon substrate, we were able to experimentally determine the SERS enhancement factor associated with the hot spot at different orientations relative to the laser polarization. To our knowledge, this work represents the first attempt to isolate the hot spot formed between two Ag nanoparticles with subsequent measurements of the SERS enhancement factor intrinsic to a hot spot.

The sharp Ag nanocubes used in our SERS studies had an edge length of 100 ± 5.7 nm (Figure S1 in the Supporting Information). We chose them for a number of reasons. For example, they can be routinely synthesized with good uniformity in terms of shape and size distribution by the polyol method.[10] Their sharp corners and relatively large dimensions ensure that we will be able to obtain strong SERS signals as compared to smaller or rounded particles.[11] Also, they represent an ideal system for the isolation of the hot spot through plasma etching. We employed 4-methylbenzenethiol (4-MBT) and 1,4-benzenedithiol (1,4-BDT) as the SERS probe molecules because they are known to form well-defined monolayers on Ag surfaces by a strong Ag–S linkage with characteristic molecular footprints. These attributes are critical to estimating the total number of molecules being probed and therefore the EF.[12] Moreover, these molecules are expected to be able to penetrate into the hot-spot region between two Ag nanocubes owing to their relatively small sizes.

We started our measurements by investigating the effect of plasma etching on individual Ag nanocubes (Figure 1a). Specifically, we wanted to know whether 4-MBT molecules adsorbed on the surface of a Ag nanocube could be removed by brief plasma etching. We were also interested in understanding if the plasma etching would lead to any physical or chemical changes to the Ag nanocube, including its capability to enhance the SERS signals from 4-MBT redeposited on the Ag nanocube. Figure 1b shows a set of SERS spectra taken from the same Ag nanocube, which was functionalized with 4-MBT, plasma etched for 2 min, and then refunctionalized with 4-MBT by immersion into its solution. With the assistance of registration marks, we were able to locate the same Ag nanocube (see the inset) and take SERS spectra from it during these steps. We also repeated the cycle of functionalization, etching, and refunctionalization a number of times to see if plasma etching would eventually cause any irreversible

[*] P. H. C. Camargo, M. Rycenga, L. Au, Prof. Y. Xia
Department of Biomedical Engineering, Washington University
Saint Louis, Missouri 63130 (USA)
E-mail: xia@biomed.wustl.edu

[**] This work was supported in part by a research grant from the NSF (DMR-0804088) and a 2006 Director's Pioneer Award from the NIH (5DP1OD000798). P.H.C.C. was supported in part by the Fulbright Program and the Brazilian Ministry of Education (CAPES).

Supporting information for this article is available on the WWW under http://dx.doi.org/10.1002/anie.200806139.

WILEY InterScience DISCOVER SOMETHING GREAT

© 2009 Wiley-VCH Verlag GmbH & Co. KGaA, Weinheim

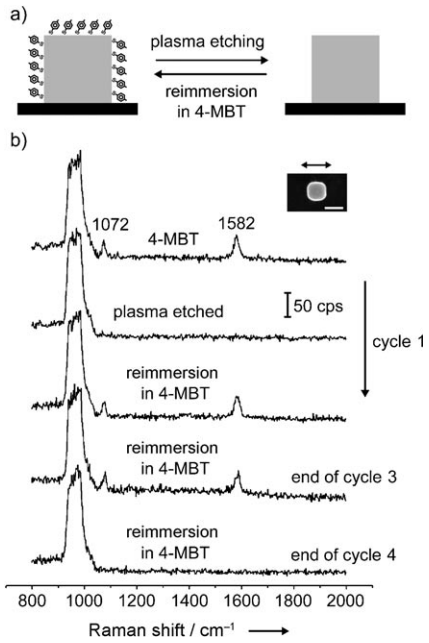

Figure 1. a) Schematic depiction of the approach employed for removal and functionalization of a single Ag nanocube with 4-MBT by plasma etching and reimmersion in a 4-MBT solution. b) SERS spectra from a single Ag nanocube functionalized with 4-MBT with subsequent successive cycles of plasma etching and reimmersion in 4-MBT (from top to bottom, respectively). The exchange process could occur up to three cycles of plasma etching and reimmersion in 4-MBT solution. After the fourth round of plasma etching, the silver nanocubes could no longer be refunctionalized with 4-MBT. The SEM image in the inset was taken after the fourth round of plasma etching; the slight truncation at corners is probably due to surface oxidation under extended exposure to the oxygen plasma. The scale bar in the inset corresponds to 100 nm, and the double arrow above it indicates the direction of laser polarization; cps = counts per second.

change to the Ag surface. As clearly shown in Figure 1b, the initial spectrum (top trace) presents the characteristic SERS peaks for 4-MBT at 1072 and 1582 cm^{-1}.[13] The nanocube was oriented with one of its edges parallel to the laser polarization. The peak at 1072 cm^{-1} is due to a combination of the phenyl ring breathing mode, CH in-plane bending, and CS stretching, while the peak at 1582 cm^{-1} can be assigned to phenyl ring stretching motion (8a vibrational mode).[14] The broad band at 900–1000 cm^{-1} came from the silicon substrate. After the sample had been plasma etched for 2 min, both the 4-MBT peaks disappeared from the SERS spectrum (second trace from the top), indicating complete removal of the 4-MBT molecules from the surface of the nanocube. Interestingly, both peaks of 4-MBT appeared again in the SERS spectrum (third trace from the top) after the etched sample had been reimmersed in the 4-MBT solution. No significant change was observed for the SERS peaks of 4-MBT when the first and third spectra were compared. This result suggests that the number of 4-MBT molecules that were redeposited on the Ag nanocube after plasma etching was essentially the same as the number of molecules initially adsorbed on the Ag nanocube. It also implies that plasma etching merely removes the 4-MBT molecules from the surface of the Ag nanocube when the exposure time is relatively short. The complete cycle of plasma etching and reimmersion in 4-MBT could be repeated up to three times without observing major deterioration in the SERS spectrum. However, after the fourth cycle, no 4-MBT peaks could be detected. It is possible that surface oxidation after extended exposure to the oxygen-based plasma will hamper the adsorption of 4-MBT onto the surface.

Plasma etching could also be employed to change the probe molecules adsorbed on the surface of an individual Ag nanocube. This concept is illustrated in Figure 2. In the first step, the nanocube is functionalized with 4-MBT. Then, the 4-MBT molecules are removed by briefly subjecting the sample to plasma etching. Finally, the sample is immersed in a solution containing 1,4-BDT. Figure 3 shows the SERS spectra recorded from a sample going through these steps. In Figure 3a, the nanocube was oriented with one of its edges parallel to the laser polarization. The initial spectrum (top trace) presents the characteristic peaks for 4-MBT at 1073 and 1583 cm^{-1},[13] which completely disappeared after plasma etching (middle trace). After immersion in a 1,4-BDT solution, the characteristic peaks for 1,4-BDT appeared in the SERS spectrum as a result of the adsorption of 1,4-BDT onto the nanocube. In this case, we observed a shift in the phenyl ring stretching motion band (8a mode) from 1582 cm^{-1} for 4-MBT to 1562 cm^{-1} for 1,4-BDT.[15] The same trend was also observed when the nanocube was orientated with one of its face diagonals parallel to the laser polarization (Figure 3b). In this case, the intensities of the SERS signals were much stronger than those in Figure 3a. As previously reported by our group, the SERS signals taken from a single Ag nanocube had a strong dependence on the laser polarization, which could be attributed to the difference in near-field distribution over the surface of a nanocube under different polarization directions.[16] In addition to the shift in position for the 8a band from 1583 to 1562 cm^{-1}, broadening

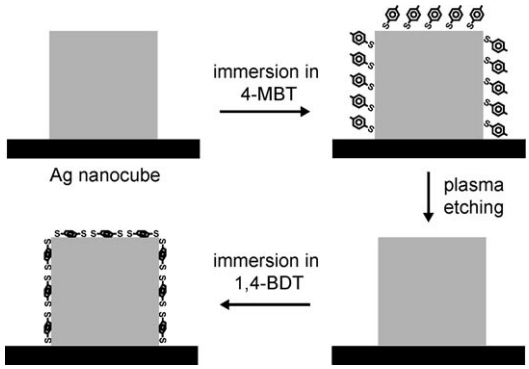

Figure 2. Schematic depiction of the approach employed for the exchange between 4-MBT and 1,4-BDT on a single Ag nanocube. The Ag nanocube is functionalized with 4-MBT and then exposed to plasma etching to remove the absorbed 4-MBT molecules from the surface of the nanocube. In the next step, the nanocube is immersed in a solution of 1,4-BDT molecules. As 4-MBT and 1,4-BDT present different Raman signatures, the exchange process can be readily monitored by observing the shift in the 8a band (1550–1600 cm^{-1}) for the benzene ring.

 © 2009 Wiley-VCH Verlag GmbH & Co. KGaA, Weinheim

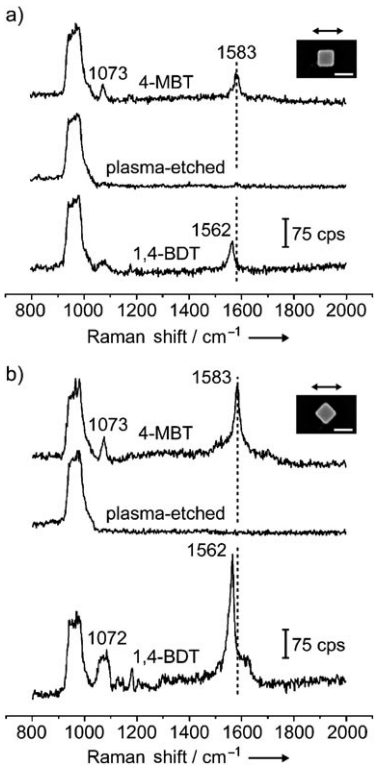

Figure 3. SERS spectra from a single Ag nanocube functionalized with 4-MBT (top trace) with subsequent plasma etching for 2 min (middle) and immersion in a 1,4-BDT solution (bottom). In (a) and (b), the laser was polarized along an edge and a face diagonal, respectively, of the Ag nanocube. The scale bar in the inset corresponds to 100 nm.

was observed for the band at 1072 cm^{-1} for 1,4-BDT as compared to 4-MBT. This broadening occurs because the ordinary Raman spectrum of 1,4-BDT displays two bands in this region (1080 and 1065 cm^{-1}), which tend to broaden and overlap in the SERS spectrum owing to interactions between the Ag surface and the π-orbital system of the benzene ring.[15] The SERS spectrum for 1,4-BDT also displayed a weak signal at 1180 cm^{-1} that could be assigned to the 9a vibrational mode (CH bending).[15]

After the experimental details for surface functionalization and plasma etching had been established for individual Ag nanocubes, we turned our attention to dimers of Ag nanocubes. In this case, we aimed at isolating the 4-MBT molecules located in the hot-spot region by exposing the sample to plasma etching under similar conditions as employed for the individual nanocubes. It is important to note that under the conditions used herein, both 4-MBT and 1,4-BDT are expected to be present on the Ag surface as a complete monolayer. Therefore, for individual Ag nanocubes, the plasma etching was responsible for the removal of a 4-MBT monolayer adsorbed on the Ag surface. Similarly, for nanocube dimers, the plasma etching is expected to remove a monolayer of 4-MBT molecules present on the surface. As the hot-spot region in the nanocube dimers comprises a narrow gap between two nearly touching nanocubes, the 4-MBT molecules in the hot spot can be considered as a multilayer resist relative to the oxygen plasma (Figure 4a). If each 4-MBT molecule has a 0.19 nm^2 footprint, each 4-MBT molecule can be assumed to occupy a circular area with a diameter of 0.49 nm on the Ag surface. As the nanocubes have an edge length of 100 nm, approximately 200 layers of 4-MBT molecules can be present in the hot-spot region along the vertical direction. Therefore, it will require a much longer time to remove the 4-MBT molecules located in the hot spot as compared to those molecules outside the hot-spot region. This scenario explains why plasma etching can serve as an effective method for isolating the hot spot formed between two Ag nanocubes. To demonstrate that no significant change took place on the surface of the nanocube dimers during plasma etching, the sample was also immersed in a 1,4-BDT solution after the hot spot had been isolated.

Figure 4b–d shows the SERS spectra from a nanocube dimer that was functionalized with 4-MBT (top trace) with subsequent plasma etching for 2 min (middle trace) and then immersion in a 1,4-BDT solution (bottom trace). In Figure 4b, the long axis of the dimer was parallel to the laser polarization. The SERS spectrum from the Ag nanocube dimer functionalized with 4-MBT clearly showed the characteristic peaks for 4-MBT at 1072 and 1582 cm^{-1}.[13,14] The much stronger intensity of the SERS signals as compared to Figures 1b and 3a reflects a higher SERS activity for the dimer relative to the individual nanocubes, owing to the presence of a hot spot. We employed the peak at 1582 cm^{-1} to estimate the EF as described in the Supporting Information. Based on our assumptions, the EF for the initial nanocube dimer (EF_{dimer}) functionalized with 4-MBT (Figure 4b, top trace) was 2.2×10^7. In comparison, the EF calculated for an individual Ag nanocube (EF_{cube}) under the same polarization (Figure 3a, top trace) was 5.9×10^5. This result indicates that EF_{dimer} was approximately 37 times higher than EF_{cube}. After plasma etching (Figure 4b, middle trace), a slight decrease in the intensity was observed for the 4-MBT bands at 1072 and 1582 cm^{-1}. This slight reduction owing to the removal of 4-MBT molecules from the region outside the hot-spot region indicates that the molecules in the hot spot were the major contributors to the SERS signals from the dimer. When it was assumed that only the 4-MBT molecules adsorbed in the hot-spot region were present in the nanocube dimer after plasma etching, the calculated EF for the hot-spot ($EF_{hot\text{-}spot}$) was 1.0×10^8. In this case, $EF_{hot\text{-}spot}$ was higher than EF_{dimer} and EF_{cube} by factors of 4.5 and 170, respectively. After the sample was immersed in a 1,4-BDT solution, all the peaks arising from 4-MBT were replaced by the characteristic peaks of 1,4-BDT (Figure 4b, bottom trace), as it can be observed from the shifting of the 8a band to 1561 cm^{-1} and the broadening of the 1073 cm^{-1} peak. This result indicates that, in addition to being adsorbed onto the faces of the nanocubes outside the hot spot, 1,4-BDT replaced the 4-MBT molecules in the hot-spot region. The stronger interaction between 1,4-BDT and Ag than 4-MBT and Ag may provide the driving force for this process (Figures S2 and S3 in the Supporting Information).[13–15,17] After complete replacement of 4-MBT by 1,4-BDT, EF_{dimer} was 1.9×10^7, which is close to the initial EF_{dimer} obtained with 4-MBT, indicating that no significant change on the surface of the nanocube dimers occurred as a result of plasma etching.

 © 2009 Wiley-VCH Verlag GmbH & Co. KGaA, Weinheim

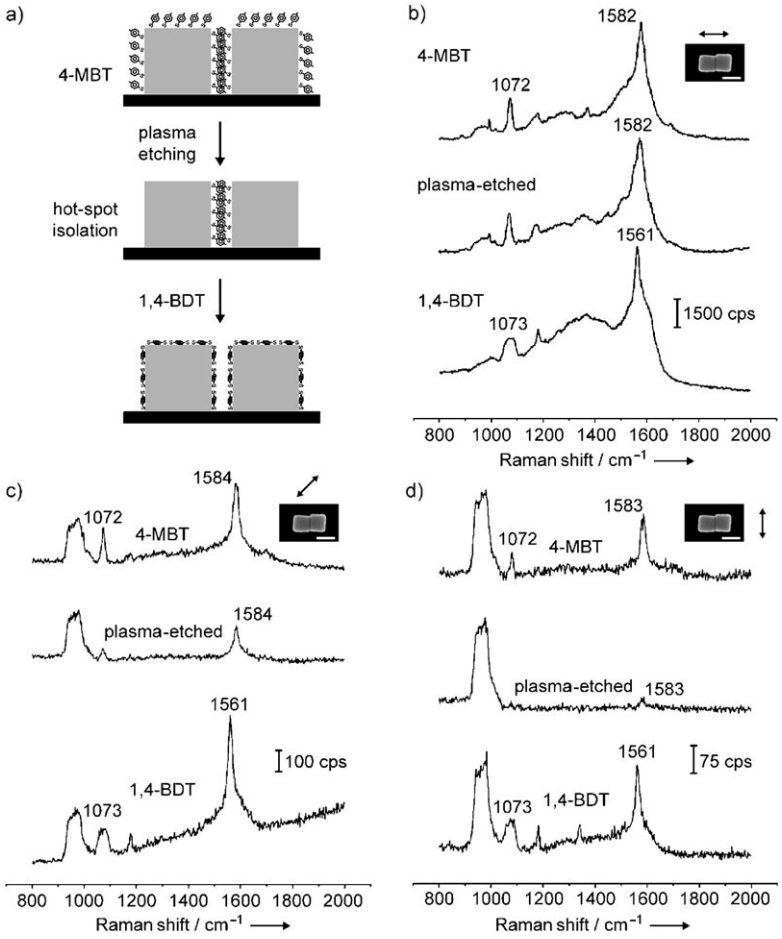

Figure 4. a) Schematic depiction of the approach employed for probing the hot spot formed in a dimer of Ag nanocubes. The dimer was functionalized with 4-MBT and then exposed to plasma etching to remove the adsorbed 4-MBT molecules. In this case, only the 4-MBT molecules outside the hot-spot region (i.e., outside the two touching faces) were removed during the plasma etching. The nanocube dimer was then immersed in a 1,4-BDT solution, resulting in the complete replacement of 4-MBT by 1,4-BDT over its entire surface. b–d) SERS spectra from a Ag nanocube dimer functionalized with 4-MBT (top) with subsequent plasma etching for 2 min (middle) and then immersion in a 1,4-BDT solution (bottom). The laser was polarized at 0, 45, and 90° with respect to the long axis of the dimer. The scale bars in the insets correspond to 100 nm.

Figure 4c illustrates the SERS spectra from the nanocube dimer in which the long axis of the dimer was at 45° relative to the laser polarization. The SERS signals were weaker than those in the spectra shown in Figure 4b as a result of inferior SERS activities in this configuration. The initial spectrum for the nanocube dimer presents the characteristic peaks for 4-MBT. EF_{dimer} was calculated as 2.0×10^6, representing an 11-fold decrease as compared to EF_{dimer} calculated from Figure 4b. In comparison, when the individual nanocube was orientated with a face diagonal parallel to the laser polarization (Figure 3b, top trace), EF_{cube} was 2.3×10^6. The fact that EF_{dimer} is close to EF_{cube} under this configuration suggests that the molecules in the hot spot did not contribute additionally towards the SERS signals observed for the dimer. This conclusion is also confirmed by inspecting the SERS spectrum after plasma etching (Figure 4c, middle trace). In this case, a significant decrease in intensity for both the 1072 and 1584 cm^{-1} peaks were observed as the 4-MBT molecules were removed from the region outside the hot spot. $EF_{hot\text{-}spot}$ was calculated to be 4.1×10^6, indicating that $EF_{hot\text{-}spot}$ is within the same order of magnitude as EF_{dimer} and EF_{cube}. After the sample was immersed in a 1,4-BDT solution, all the peaks arising from 4-MBT were replaced by the characteristic peaks of 1,4-BDT (Figure 4c, bottom trace), and EF_{dimer} was calculated as 1.6×10^6, which agrees with the initial EF_{dimer} obtained with 4-MBT.

Figure 4d shows the SERS spectra for which the long axis of the dimer was perpendicular to the laser polarization direction. In this case, the intensity of the SERS signals further decreased in comparison to Figure 4c, and they were much weaker relative to Figure 4b. EF_{dimer} was calculated as 6.8×10^5, which is close to the value of 5.9×10^5 obtained for single Ag nanocubes (Figure 3a), suggesting that the molecules in the hot spot did not make any additional contribution toward SERS signals observed for the dimer. After plasma etching, while the peak at 1072 cm^{-1} completely disappeared, the peak at 1583 cm^{-1} became very weak and $EF_{hot\text{-}spot}$ became 4.4×10^5, which was on the same order of magnitude as EF_{dimer} and EF_{cube}. After immersion in 1,4-BDT, all the 4-MBT signals were replaced by the characteristic peaks of 1,4-BDT, and EF_{dimer} was found to be 5.4×10^5.

According to near-field calculations by the discrete-dipole approximation (DDA) method for Ag nanocubes 100 nm in size at 514 nm excitation,[16] the near-field distribution is expected to be concentrated on the faces that form the hot-spot region when the laser polarization is parallel to the dimer long axis. This arrangement could lead to a SERS enhancement of 170-fold stronger for $EF_{hot\text{-}spot}$ as compared to EF_{cube}. However, when the long axis of the dimer is at 45 and 90° relative to the laser polarization direction, the near-field distributions are expected to be mostly concentrated outside the hot-spot region, that is, at the corners and on the faces that are perpendicular to the dimer's long axis, respectively. This reduction of near-field distribution in the hot-spot region can be considered to be responsible for the significant decrease in $EF_{hot\text{-}spot}$ when the long axis of the dimer is at 45 and 90° relative to the laser polarization.

In summary, we have demonstrated a simple and versatile approach based on plasma etching for isolating and exclusively probing the hot spot in a dimer of Ag nanocubes. In this approach, the dimer of Ag nanocubes was first functionalized with 4-MBT and the hot spot was then isolated by exposing the sample to plasma etching. The plasma etching only led to the removal of molecules adsorbed on the surface outside the hot-spot region. Finally, the sample was functionalized with 1,4-BDT to demonstrate that the surface of the dimer did not

 © 2009 Wiley-VCH Verlag GmbH & Co. KGaA, Weinheim

undergo any significant changes during plasma etching. Based on this approach, $EF_{hot\text{-}spot}$ was calculated as 1.0×10^8, 4.1×10^6, and 4.4×10^5 as the long axis of the dimer was oriented at 0 (parallel), 45, and 90° (perpendicular), respectively, relative to the laser polarization. Likewise, EF_{dimer} (without isolating the hot spot) was calculated as 2.2×10^7, 2.0×10^6, and 6.8×10^5, respectively. These results indicate that $EF_{hot\text{-}spot}$ displayed a strong dependence on the laser polarization, experiencing an increase by factors of approximately 10 and 230 as the long axis of the dimer was rotated from 90 to 45° and from 90 to 0° (relative to the laser polarization). Similarly, EF_{dimer} displayed increases by factors of approximately 3 and 30. By comparing $EF_{hot\text{-}spot}$ with EF_{cube}, $EF_{hot\text{-}spot}$ was increased by approximately 170-fold when the dimer's long axis was parallel to the direction of laser polarization.

Experimental Section

The Ag nanocubes were synthesized according to our previously reported procedures.[10] Samples for correlated SEM and SERS experiments were prepared by drop-casting an ethanol suspension of the Ag nanocubes on a silicon substrate that had been patterned with registration marks and letting it dry under ambient conditions. In this case, dimers could form spontaneously by aggregation during solvent evaporation. Functionalization with 4-methylbenzenethiol (4-MBT, Aldrich) or 1,4-benzenedithiol (1,4-BDT, Aldrich) was performed by immersing the substrate containing Ag nanocubes in a 5 mM ethanol solution (5 mL) of 4-MBT or 1,4-BDT, respectively, for 1 h. The sample was then taken out, washed with copious amounts of ethanol, and finally dried under a stream of nitrogen. The plasma etching was performed in a plasma cleaner/sterilizer (Harrick Scientific Corp., PDC-001) operated at 60 Hz and 0.2 Torr air, with power being set to high. Plasma etching of the sample was performed by placing the Si substrate containing the Ag particles in the plasma cleaner chamber and exposing it to the oxygen plasma for 2 min. Since plasma etching is highly sensitive to many parameters, at least the etching time and air pressure must be optimized when this protocol is applied to a specific system. All samples were used immediately for SERS measurements after preparation. The SERS spectra for individual Ag nanocubes and dimers were monitored after each step of functionalization and plasma etching.

Received: December 16, 2008
Published online: February 6, 2009

Keywords: hot spots · nanocubes · Raman spectroscopy · silver · surface plasmon resonance

[1] a) S. Nie, S. R. Emory, *Science* **1997**, *275*, 1102; b) K. Kneipp, Y. Wang, H. Kneipp, L. T. Perelman, I. Itzkan, R. R. Dasari, M. S. Feld, *Phys. Rev. Lett.* **1997**, *78*, 1667.
[2] Recent reviews: a) N. P. W. Pieczonka, R. F. Aroca, *Chem. Soc. Rev.* **2008**, *37*, 946; b) P. L. Stiles, J. A. Dieringer, N. L. Shah, R. P. Van Duyne, *Annu. Rev. Anal. Chem.* **2008**, *1*, 601; c) K. A. Willets, R. P. Van Duyne, *Annu. Rev. Phys. Chem.* **2007**, *58*, 267; d) K. Kneipp, H. Kneipp, J. Kneipp, *Acc. Chem. Res.* **2006**, *39*, 443.
[3] a) A. Otto, *J. Raman Spectrosc.* **2006**, *37*, 937; b) E. C. Le Ru, P. G. Etchegoin, M. Meyer, *J. Chem. Phys.* **2006**, *125*, 204701; c) W. E. Doering, S. Nie, *J. Phys. Chem. B* **2002**, *106*, 311.
[4] a) E. C. Le Ru, M. Meyer, E. Blackie, P. G. Etchegoin, *J. Raman Spectrosc.* **2008**, *39*, 1127; b) E. C. Le Ru, E. Blackie, M. Meyer, P. G. Etchegoin, *J. Phys. Chem. C* **2007**, *111*, 13794; c) Z. Wang, S. Pan, T. D. Kraus, H. Du, L. J. Rotheberg, *Proc. Natl. Acad. Sci. USA* **2003**, *100*, 8638; d) A. Otto, *J. Raman Spectrosc.* **2002**, *33*, 593.
[5] K. Kneipp, H. Kneipp, I. Itzkan, R. R. Dasari, M. S. Feld, *Chem. Rev.* **1999**, *99*, 2957.
[6] a) P. Olk, J. Renger, T. Härtling, M. T. Wenzel, L. M. Eng, *Nano Lett.* **2007**, *7*, 1736; b) F. Svedberg, Z. Li, H. Xu, M. Käll, *Nano Lett.* **2006**, *6*, 2639.
[7] a) C. E. Talley, J. B. Jackson, C. Oubre, N. K. Grady, C. W. Hollars, S. M. Lane, T. R. Huser, P. Nordlander, N. J. Halas, *Nano Lett.* **2005**, *5*, 1569; b) D. W. Brandl, C. Oubre, P. Nordlander, *J. Chem. Phys.* **2005**, *123*, 024701; c) H. Wang, N. J. Halas, *Nano Lett.* **2006**, *6*, 2945.
[8] W. Li, P. H. C. Camargo, X. Lu, Y. Xia, *Nano Lett.* **2009**, *9*, 485.
[9] J. P. Camden, J. A. Dieringer, Y. Wang, D. J. Masiello, L. D. Marks, G. C. Schatz, R. P. Van Duyne, *J. Am. Chem. Soc.* **2008**, *130*, 12616.
[10] a) S. E. Skrabalak, L. Au, X. Li, Y. Xia, *Nat. Protoc.* **2007**, *2*, 2182; b) S. H. Im, Y. T. Lee, B. Wiley, Y. Xia, *Angew. Chem.* **2005**, *117*, 2192; *Angew. Chem. Int. Ed.* **2005**, *44*, 2154; c) Y. Sun, Y. Xia, *Science* **2002**, *298*, 2176.
[11] a) J. M. McLellan, A. Siekkinen, J. Chen, Y. Xia, *Chem. Phys. Lett.* **2006**, *427*, 122; b) E. Hao, G. C. Schatz, *J. Chem. Phys.* **2004**, *120*, 357.
[12] A. D. McFarland, M. A. Young, J. A. Dieringer, R. P. Van Duyne, *J. Phys. Chem. B* **2005**, *109*, 11279.
[13] a) M. A. Khan, T. P. Hogan, S. Shanker, *J. Raman Spectrosc.* **2008**, *39*, 893; b) G. Sauer, G. Brehm, S. Schneider, *J. Raman Spectrosc.* **2004**, *35*, 568.
[14] a) M. Osawa, N. Matsuda, K. Yoshii, I. Uchida, *J. Phys. Chem.* **1994**, *98*, 12702; b) J. Y. Gui, D. A. Stern, D. G. Frank, F. Lu, D. C. Zapien, A. T. Hubbard, *Langmuir* **1991**, *7*, 955.
[15] a) S. W. Joo, S. W. Han, K. Kim, *J. Colloid Interface Sci.* **2001**, *240*, 391; b) S. H. Cho, H. S. Han, D. J. Jang, K. Kim, M. S. Kim, *J. Phys. Chem.* **1995**, *99*, 10594.
[16] J. M. McLellan, Z. Y. Li, A. R. Siekkinen, Y. Xia, *Nano Lett.* **2007**, *7*, 1013.
[17] K. Seo, E. Borguet, *J. Phys. Chem. C* **2007**, *111*, 6335.

 © 2009 Wiley-VCH Verlag GmbH & Co. KGaA, Weinheim